Published in final edited form as:
Cancer Discov. 2014 January ; 4(1): 42–52. doi:10.1158/2159-8290.CD-13-0315.

mTOR Inhibition Specifically Sensitizes Colorectal Cancers with KRAS or BRAF Mutations to BCL-2/BCL-XL Inhibition by Suppressing MCL-1

Anthony C. Faber[1,2,*], **Erin M. Coffee**[3,*,#], **Carlotta Costa**[1,2], **Anahita Dastur**[1,2], **Hiromichi Ebi**[1,2,Ω], **Aaron N. Hata**[1,2], **Alan T. Yeo**[1,2], **Elena J. Edelman**[1,2], **Youngchul Song**[1,2], **Ah Ting Tam**[1,2], **Jessica L. Boisvert**[1,2], **Randy J. Milano**[1,2], **Jatin Roper**[3], **David P. Kodack**[2,4], **Rakesh K. Jain**[2,4], **Ryan B. Corcoran**[1,2], **Miguel N. Rivera**[1,2,5], **Sridhar Ramaswamy**[1,2], **Kenneth E. Hung**[3,+], **Cyril H. Benes**[1,2], and **Jeffrey A. Engelman**[1,2]

[1]Massachusetts General Hospital Cancer Center, Boston, MA 02129, USA

[2]Department of Medicine, Harvard Medical School, Boston, MA 02115, USA

[3]Tufts Medical Center, Department of Medicine, Division of Gastroenterology, Boston, MA 02111, USA

[4]Radiation Oncology, Steele Lab for Tumor Biology, Massachusetts General Hospital and Harvard Medical School, Charlestown, MA 02129, USA

[5]Department of Pathology, Massachusetts General Hospital, Boston, MA 02114, USA

Abstract

Colorectal cancers (CRCs) harboring *KRAS* or *BRAF* mutations are refractory to current targeted therapies. Using data from a high-throughput drug screen, we have developed a novel therapeutic strategy that combines targeting of the apoptotic machinery using the BCL-2 family inhibitor ABT-263 (navitoclax) in combination with a TORC1/2 inhibitor, AZD8055. This combination leads to efficient apoptosis specifically in *KRAS* mutant (MT) and *BRAF* MT but not wild-type (WT) CRC cells. This specific susceptibility results from TORC1/2 inhibition leading to suppression of MCL-1 expression in mutant, but not WT CRCs, leading to abrogation of BIM/MCL-1 complexes. This combination strategy leads to tumor regressions in both *KRAS* MT colorectal cancer xenograft and genetically-engineered mouse models of CRC, but not in the corresponding *KRAS* WT CRC models. These data suggest that the combination of BCL-2/XL inhibitors with TORC1/2 inhibitors constitutes a promising targeted therapy strategy to treat these recalcitrant cancers.

Keywords

KRAS; BRAF; colorectal cancer; targeted therapy; ABT-263

Reprint requests should be sent to Jeffrey Engelman, Massachusetts General Hospital, 149 13th Street, Rm. 7316, Boston, MA 02129.
[*]denotes equal contribution
[#]current address is Massachusetts General Hospital Cancer Center, Boston, MA, USA
[Ω]current address is Cancer Research Institute, Kanazawa University, Kanazawa, Japan
[+]current address is Department of Precision Medicine, Biotherapeutics, Pfizer, Inc., Cambridge MA, USA

There are no conflicts of interest to disclose

Introduction

KRAS mutations are observed in ~ 30–45% of CRCs (1–3). These mutations lead to potent activation of the MEK-ERK signaling pathway (4). Although therapies targeting EGFR have some efficacy in CRCs without *KRAS* mutations (1, 5–8), these therapies most likely fail because the MEK-ERK pathway is sustained by mutant KRAS in the presence of EGFR inhibitory antibodies. Direct inhibitors of mutant KRAS protein are not yet available; therefore, efforts are often focused on targets in signaling pathways whose inhibition alone or in combination may be effective for this subset of cancers (9–16). Indeed, multiple approaches, including the combination of PI3K and MEK pathway inhibitors, are being examined in clinical trials. Mutant BRAF, which is directly downstream of KRAS, also leads to hyperactivation of the MEK-ERK pathway. *BRAF* mutations occur in roughly 5–15% of CRCs (1–3, 17), and are generally mutually exclusive with *KRAS* mutations (1). In fact, a recent report highlighted gene expression similarities in these two genetically distinct MT CRCs, underscoring the overlap in signaling downstream from these mutant oncogenes (18). Single-agent BRAF inhibitors have been largely ineffective in *BRAF* MT CRCs (19), despite activity in *BRAF* MT melanomas (20). However, some laboratory models of *BRAF* mutant CRCs are sensitive to the combination of BRAF and receptor tyrosine kinase inhibitors, particularly EGFR, and this approach is currently under evaluation in the clinic (21, 22). While some of these novel therapeutic strategies for *KRAS* and *BRAF* MT CRCs being explored in clinical trials will hopefully demonstrate some activity, it is very likely that clinical resistance will emerge, necessitating additional treatment strategies. Thus, there continues to be an urgent need to develop additional targeted therapies for *KRAS* MT as well as *BRAF* MT CRCs.

We sought to uncover targeted therapy strategies that demonstrate specificity towards *KRAS* or *BRAF* MT CRCs compared to their WT counterparts. We leveraged the results from a high-throughput screen that assessed the sensitivity of over 1,000 cell lines to more than 130 drugs (23). Since the induction of both apoptosis and growth arrest is a hallmark of many successful targeted therapy approaches (24–26), we built upon the screen results and further mechanistic insights to establish a combination strategy producing these biological effects.

Results

Data obtained from our recently described high-throughput drug screen (23, 27) allowed us to compare the efficacy of drugs between *KRAS* MT and *BRAF* MT human CRCs versus WT human CRCs. Included among the large number of compounds in the drug screen was ABT-263, a BCL-2/XL inhibitor (BH3 mimetic) that has demonstrated pre-clinical efficacy in some tumors (28, 29) and is under clinical evaluation as a single agent or in combination with chemotherapy (30, 31). In this study, we found that ABT-263 had similar activity in *KRAS* and *BRAF* MT compared to WT CRCs (Fig. 1A). In contrast to ABT-263, a different BH3 mimetic, obatoclax, neutralizes another BCL-2 family member, MCL-1, in addition to BCL-2 and BCL-XL (32). Unlike ABT-263, obatoclax was more effective in both *KRAS* and *BRAF* MT CRCs than in WT CRCs (Fig. 1B). The selectivity of obatoclax for MT CRCs was notable as many common chemotherapies and experimental therapies did not discriminate between the MT and WT CRCs (Sup. Fig.1, P=NS for all comparisons). The differential sensitivity to obatoclax was not explained simply by expression levels of either MCL-1 or other BCL-2 family members (Sup. Fig. 2A, 2B). Consistent with the increased sensitivity of MT CRCs to obatoclax, RNAi knockdown of *MCL-1* sensitized MT CRCs, but not WT CRCs, to ABT-263 (Fig. 1C, Sup. Fig. 2C). In total, these findings suggest that, in comparison to their WT counterparts, MT cells have a heightened sensitivity to combined inhibition of MCL-1, BCL-XL, and BCL-2.

These data indicated that targeting BCL-2, BCL-XL, *and* MCL-1 may be an effective therapeutic strategy in MT CRCs. However, obatoclax has significant toxicity, possibly off-target, limiting its clinical utility (33–35). Furthermore, many effective targeted therapies lead to both apoptosis and growth arrest, and inhibition of BCL-2 family members might be expected to induce apoptosis (29), but fail to strongly impair proliferation. Thus, we sought an alternative approach to both induce apoptosis and concomitantly block proliferation. Previous studies had demonstrated that efficient translation of *MCL-1* mRNA requires cap-dependent translation in some cancers (36–38). TORC1 inhibition, via loss of 4EBP1 (also referred to as EIF4EBP1) phosphorylation, results in a decrease of MCL-1 protein expression in these cancers (37–40). Consistent with those results, we found that treatment of *KRAS* MT and *BRAF* MT CRCs with the TORC1/2 inhibitor, AZD8055 (41), led to a decrease in MCL-1 expression (Fig. 1D, Sup. Fig. 2D and Sup. Fig 3). Interestingly, AZD8055 did not substantially suppress MCL-1 expression in *KRAS* and *BRAF* WT cells (Fig. 1E). Indeed, the regulation of MCL-1 expression by TORC1/2 appeared to be different between WT and MT CRCs since AZD8055 effectively suppressed TORC1 and TORC2 in both genetic backgrounds as measured by its effect on phospho-RPS6, phosho-4EBP1 and phospho-AKT at residue 473 (Fig. 1D,E). Consistent with this, treatment with AZD8055 led to a G_1 arrest in both WT and MT CRC, and thus MT and WT CRCs had similar sensitivities to single-agent AZD8055 (Sup. Fig. 4A,B). The suppression of MCL-1 protein expression by AZD8055 in MT cells was not associated with a decrease in *MCL-1* RNA levels (Sup. Fig. 5A), consistent with an effect on translation of the *MCL-1* mRNA in these cancers. Furthermore, *MCL-1* mRNA levels only slightly increased in both MT and WT cells following AZD8055 treatment, suggesting there is no differential feedback of *MCL-1* transcription contributing to differences in MCL-1 protein expression between the cancer types (Sup. Fig 5A). A time-course of AZD8055 treatment in MT cells demonstrated clear suppression of MCL-1 protein expression within two hours of treatment (Sup. Fig. 5B). In contrast, MCL-1 expression was not diminished in WT cells at any time point examined (Sup. Fig 5B).

Since TORC1/2 inhibition effectively suppressed MCL-1 expression in *KRAS* or *BRAF* MT cells, we explored whether TORC1/2 inhibitors would combine with ABT-263 to induce apoptosis specifically in these genetic backgrounds (analogous to MCL-1 siRNA sensitizing to ABT-263, Fig. 1C). It is notable that ABT-263 usually induces expression of MCL-1, and that the differential effects of AZD8055 on the expression of MCL-1 between MT and WT cells were often more dramatic when AZD8055 was combined with ABT-263 (Fig. 1D, E, Sup. Fig. 2D and Sup. Fig. 3). We assessed the induction of apoptosis across a panel of human MT and WT CRC cell lines. In addition to human cancer cell lines, we also included *ex vivo* mouse cell lines derived from CRCs induced in *KRAS* MT (*KRAS/APC/p53)* and WT (*APC/p53*) genetically-engineered mouse models (GEMMs) of CRC (42, 43). The combination of ABT-263 and AZD8055 induced substantial apoptosis in the MT human and murine CRCs (average apoptosis 59.4 ± 4.0%) (Fig. 2A). In contrast, marked apoptosis was not observed in any of the WT CRC cell lines (average apoptosis 12.5 ± 2.6%) (Fig. 2A). We also compared the effect of this combination on a pair of isogenic HCT-116 cell lines with and without KRAS mutations(44) We observed that the *KRAS* MT HCT-116 cells had approximately a seven-fold increase in apoptosis following combination therapy compared to the *KRAS* WT HCT-116 cells (Fig. 2B). Of note, MCL-1 levels decreased significantly more following AZD8055 (and the AZD8055/ABT-263 combination) in MT cells compared to the WT cells (Fig. 2C, ten-fold versus two-fold, respectively). In total, these findings support the notion that MT CRCs may be particularly more sensitive to this combination than their WT counterparts.

These findings prompted us to further examine the regulation of MCL-1 in *KRAS* MT cancers and the mechanism by which its inhibition synergized with ABT-263 to promote

apoptosis. Knockdown of *KRAS* using inducible shRNA was sufficient to suppress 4EBP1 phosphorylation, and accordingly, MCL-1 in *KRAS* MT SW620 cells (Fig. 3A). However, MEK inhibition alone did not suppress phosphorylation of 4EBP1, and accordingly, it did not decrease expression of MCL-1 (Fig. 3B). This finding is consistent with a report suggesting that other KRAS-regulated pathways, in addition to MEK-ERK, contribute to phosphorylation of 4EBP1(45). In contrast, *KRAS* knockdown did not decrease MCL-1 levels in *KRAS* WT CW-2 cells (Sup. Fig. 5C).

We further interrogated the molecular mechanisms by which the combination of TORC1/2 and BCL-2/XL inhibitors led to apoptosis in the MT cancers. To determine if the induction of apoptosis by the AZD8055/ABT-263 combination was indeed dependent on the suppression of MCL-1 expression, we expressed exogenous MCL-1 via lentiviral gene delivery. As expected, the exogenous expression of MCL-1 suppressed the induction of apoptosis (Fig. 3C, Sup. Fig. 6A). To understand how the drug combination impacted the protein complexes of the BCL-2 family, we performed immunoprecipitations in the absence and presence of inhibitors. Previous studies have shown that BIM plays a critical role in BH3 mimetic (including ABT-263)-induced apoptosis (46, 47). Analysis of immunoprecipitated BIM and MCL-1 complexes revealed that ABT-263 treatment abrogated the interaction between BIM and BCL-XL. However, ABT-263 treatment led to a proportional increase in the association between MCL-1 and BIM (Fig. 3D). These findings suggest that the BIM released from BCL-2 and BCL-XL in response to ABT-263 was bound to MCL-1, preventing apoptosis. Adding AZD8055 to ABT-263 resulted in loss of BIM/MCL-1 complexes (Fig. 3D) corresponding to decreases of MCL-1 expression in the whole cell extracts (Fig. 3D). AZD8055 treatment also led to reduced complexes between MCL-1 and BAK due to loss of MCL-1 (Fig. 3D, middle panel), likely contributing to the amount of apoptosis induced by the combination. In *KRAS* WT cells, analysis of immunoprecipitated BIM complexes revealed that, similar to the *KRAS* MT cells, ABT-263 treatment blocked the interaction between BIM and BCL-XL, and that treatment led to a proportional increase in the association between MCL-1 and BIM. However, in contrast to the MT cells, AZD8055 treatment did not reduce BIM/MCL-1 complexes (Sup. Fig. 6B), consistent with the lack of reduction of MCL-1 following AZD8055 treatment in the total cell lysates (Sup. Fig. 6B) and the lack of efficacy of the combination (Fig. 2A). A model depicting the impact of the combination on the BCL-2 family is shown in Fig. 3E. Of note, this mechanism of apoptosis is distinct from the recently described combination of ABT-263 and MEK inhibitor(16), AZD6244. Unlike AZD8055, the MEK inhibitor does not decrease levels of MCL-1, but rather increases levels of BIM (Fig. 3D).

Next, we asked whether our findings in MT CRCs extended to another type of *KRAS* mutant cancer, *KRAS* MT non-small cell lung cancers (NSCLCs). In contrast to *KRAS* MT CRC, AZD8055 failed to markedly downregulate MCL-1 in *KRAS* MT NSCLC cell lines (Sup. Fig. 7A), and accordingly, it failed to substantially increase the amount of apoptosis induced by ABT-263 in the NSCLC cell lines (Sup. Fig. 7B). However, NSCLC cells were highly sensitive to ABT-263 treatment following *MCL-1* knockdown (Sup. Fig. 7C), suggesting *KRAS* MT cancers in general may be sensitive to simultaneous BCL-2, BCL-XL and MCL-1 inhibition, but that TORC1 regulation of MCL-1 may be different between *KRAS* MT CRC and *KRAS* MT NSCLC. In support of this hypothesis, AZD8055 treatment led to a modest increase in the level of *MCL-1* transcript in *KRAS* MT NSCLCs (Sup. Fig. 7D), similar to *KRAS* MT CRCs and *KRAS* WT CRCs (Sup. Fig 5A). Furthermore, KRAS knockdown in *KRAS* mutant H2009 and H358 cells failed to significantly downregulate MCL-1 expression (Sup. Fig. 7E) in contrast to KRAS knockdown in *KRAS* mutant SW620 cells (Fig. 3A). Of note, we did not detect any differences between the stability of MCL-1 protein between *KRAS* MT CRC and *KRAS* MT NSCLC cell lines, as determined by Western blotting of MCL-1 following a short-term time-course of treatment with the protein translational

inhibitor, cycloheximide (Sup. Fig. 8). Altogether, these data suggest that MCL-1 may be an important survival signal for *KRAS* MT cancers in general, however, the regulation of MCL-1 expression by TORC1/2 is not equivalent in *KRAS* MT NSCLCs.

Since the ABT-263/AZD8055 combination in *KRAS* MT CRCs induces both apoptosis (Fig. 2A) and growth arrest (Sup. Fig. 4A), we evaluated this therapeutic strategy *in vivo* against established *KRAS* MT CRCs. In a SW620 *KRAS* MT CRC xenograft tumor model, combination treatment resulted in marked tumor growth impairment, and even some regressions (Fig. 4A, *left panel*). AZD8055 downregulated MCL-1 and there was a marked induction of cell death following combination therapy *in vivo* (Fig. 4B, Sup. Fig. 9A). Notably, SW620 tumors have been resistant to several other combination approaches in clinical development, highlighting the potential of the current approach (Sup. Fig. 9B). As expected, the combination of AZD8055/ABT-263 failed to significantly prevent tumor growth or suppress MCL-1 expression in a *KRAS* WT xenograft tumor model (Fig. 4A, *right panel*, Fig. 4B). Thus, this combination demonstrated more impressive activity against the *KRAS* mutant CRC *in vivo*, consistent with the *in vitro* data.

We next tested this combination in genetically engineered mouse models (GEMMs) of *KRAS* MT and *KRAS* WT CRC. These GEMMs are valuable preclinical models. In contrast to xenograft cancer models, the GEMM tumors develop in the physiologically relevant microenvironment of the colon and do not undergo growth selection *in vitro* prior to *in vivo* testing (42). Furthermore, the ability to monitor tumor growth and/or regressions using optical colonoscopy allows us to follow the dynamic tumor responses to treatment in real time, making this model particularly valuable and effective for evaluating experimental therapeutics. We examined the efficacy of the combination regimen on mice with colonic tumors that were *APC* mutant (null) (48) with or without *KRAS* mutation (42). The growth or regressions of individual tumors were monitored weekly by serial colonoscopies (42). The *KRAS* MT CRC model treated with combination therapy exhibited shrinkage of all treated tumors (Fig. 4C,D). In contrast, the combination failed to induce tumor regressions in *KRAS* WT GEMMs (Fig. 4C,D), despite effective inhibition of TORC1/2 signaling *in vivo* (Fig. 4E). Therefore, GEMMs of CRC reflect our findings in human CRC cell lines assessed *in vitro* and as xenografts *in vivo*, further supporting the efficacy and specificity of this regimen for *KRAS* MT CRCs.

Discussion

Advanced CRCs with *KRAS* or *BRAF* mutations require new therapeutic options. Here, we show that combining AZD8055 with ABT-263 induces robust apoptosis in *KRAS* and *BRAF* MT human CRC cell lines. Further, this combination produced tumor regressions in *KRAS* MT CRCs *in vivo* both in human xenografts and in GEMMs, increasing the likeliness that this combination may have efficacy in clinical trials of *KRAS* MT CRCs. While our initial observation that *KRAS* and *BRAF* MT CRCs had enhanced sensitivity to single-agent obatoclax compared to their WT counterparts, we believe that this combination is likely to be preferable to obatoclax for two main reasons: 1) BH3 mimetics alone induce apoptosis but do not appear to induce growth arrest, and 2) clinical trial data suggest that the dose-limiting toxicities of obatoclax may preclude sufficient target inhibition, in contrast to ABT-263 (30, 34, 35). Furthermore, we are optimistic that this combination may have an attractive therapeutic index. Doses of AZD8055 as low as ~17nM effectively reduced MCL-1 levels and sensitized the cells to ABT-263 (Sup. Fig. 10A,B). Even when we decreased the concentrations of AZD8055 *in vivo* from 16mg/kg to 2mg/kg, significant tumor inhibition in the SW620 model was still achieved (Sup. Fig.10C).

Recently, there have been a number of studies that have sought effective approaches to treat *KRAS* mutant cancers. These therapies include MEK inhibition in combination with BCL-2/XL inhibition (16), STK33 inhibition (13), TAK1 inhibition (14), MEK inhibition in combination with PI3K inhibition (11), GATA2 inhibition (15, 49), CDC6 inhibition (49), APC/C inhibition (50) and PLK1 inhibition (50). At this point, it is difficult to predict which approaches will ultimately emerge as effective therapies in the clinic, and potential therapeutic indices for each of these therapies have yet to be established. This will likely have a large impact on determining which approaches have greatest clinical value. In addition, there may be different subsets of *KRAS* mutant cancers that are susceptible to a particular combination. As an example, the combination of a MEK inhibitor with a BCL-2/XL inhibitor demonstrated efficacy across a large swath of *KRAS* mutant cancers, including *KRAS* mutant lung cancers, but tended to be less effective in *KRAS* mutant cancers with mesenchymal features (16). In contrast, the combination of AZD8055 with a BCL-2/XL inhibitor appeared less active against *KRAS* MT lung cancers, but demonstrated potency against all *KRAS* MT CRCs examined.

The current study offers some unique components that may facilitate drug development. Most published studies utilized RNA interference approaches to identify potential therapeutic strategies, and thus further drug development efforts will be necessary to achieve clinical translation. The current study differs in that we utilized data from a high- throughput drug screen involving clinically relevant inhibitors to identify a treatment strategy specific for *KRAS* MT CRC. Although our current approach restricts the number of targets being explored (compared to comprehensive RNA interference screens), it is rather straightforward to examine the efficacy of this drug combination in the clinic relatively quickly.

The combination developed in this study for *KRAS* MT CRCs is less active in *KRAS* WT CRCs. The activity of this combination centers on the sensitization of these cancers to ABT-263 by suppression of MCL-1 expression upon treatment with TORC1/2 inhibitors. In contrast to the *KRAS* mutant CRCs, the WT CRCs were not sensitized to ABT-263 by downregulation of MCL-1 *nor* did they have MCL-1 expression under the regulation of TORC. Although further studies will be required to determine the activity of this combination in other subsets of cancer, we speculate that this combination may be effective for cancers that have MCL-1 expression under strict regulation of the TORC1 pathway and are sensitive to simultaneous BCL-2/BCL-XL/MCL-1 disruption.

Overall, we believe that the combination of TORC inhibitors with BCL-2/XL inhibitors are mechanistically designed to induce apoptosis and growth arrest in the subset of CRCs with *KRAS* or *BRAF* mutations and warrants further investigation as a potential clinical treatment for these recalcitrant cancers.

MATERIALS AND METHODS

Cell Lines

All of the cell lines used in this study were provided by the Center for Molecular Therapeutics (CMT) at Massachusetts General Hospital, with the exception of the genetically engineered mouse model cell lines (42) and the HCT-116 isogenic cell lines (44). The cell lines from CMT routine undergo cell line authentication testing by SNP and STR analysis. These cell lines have been acquired over the past five years. Limited genotyping of human colorectal cell lines used in the drug screen is available in Supp. Table 1. The human colorectal cell lines used in Western blotting, apoptosis assays and cell cycle assays were grown in DMEM with 10% FBS in the presence of 1ug/ml penicillin and streptomycin, expect the *BRAF* mutant COLO-205 and LS-411N cell lines which were

grown in RPMI with 10% FBS. The *KRAS* mutant lung cancer cell lines (H2009, H460, H2030 and H358) were grown in RPMI with 10% FBS.

Drug Screen

The drug screen has previously been described (23) as has the website for publically accessible drug-sensitivity data (27) (www.cancerRxgene.org). Data analysis was performed using data sets available in early 2013 and these data are recorded in Supplemental Table 1.

Antibodies and Reagents

The following antibodies were used for Western blot analyses: phospho-AKT (473) (cat #9271), phospho-RPS6 (240/244) (cat #2211), phospho-4EBP1 (cat #2855), phospho-ERK (cat #9101), total RPS6 (cat #2217), phospho-4EBP1 (cat #2855), BIM (cat #2819), BAK (cat #3814) and BCL-XL (cat #2762) were from Cell Signaling (Beverly, MA). MCL-1 (S-19) antibody was from Santa Cruz Biotechnology (Santa Cruz, CA). Antibody to glyceraldehyde-3-phosphate dehydrogenase (GAPDH) was purchased from Chemicon. Annexin-Cy5 was from Biosource International, Camarillo, CA. Propidium iodide was from Sigma-Aldrich. Opti-MEM was from Invitrogen (Carlsbad, CA). Protein A sepharose beads were from Amersham (GE Healthcare).

Western Blotting

For Western blotting of cellular lystates, cells were resuspended in lysis buffer (20 mM Tris, 150 mM NaCl, 1% Nonidet P-40, 0.1 mM EDTA, and protease and phosphatase inhibitors), incubated on ice for 10 m and centrifuged at 14,000 rpm for 10 minutes. For whole tumor lysates, these were prepared by homogenization with a TH tissue homogenizer (Omni International) in tissue lysis buffer (25mM Tris-HCl (pH 7.6), 150mM NaCl, 1% NP-40, 1% sodium deoxycholate, 0.1% SDS, 1mM DTT, and protease and phosphatase inhibitors), incubated for 10 minutes on ice, vigorously shaken for 30 minutes at 4 °C at 1400 rpm in a thermomixer and centrifuged at 14,000 rpm for 10 minutes at 4 °C. Protein concentration was determined by BCA Protein Assay (Pierce). Proteins were resolved using the NuPAGE® Novex® Midi Gel system on 4% to 12% Bis-Tris Gels (Invitrogen), transferred to nylon membranes and probed with the antibodies listed above. Representative blots are shown from several experiments. Chemiluminescence was detected with the Syngene G:Box camera (Synoptics). All measurements were performed in the linear range without saturation and were normalized to GAPDH or ACTIN loading control.

Apoptosis

Cells were seeded at roughly 30–40% confluency and cells were treated for the indicated times with the indicated treatments, with no-treatment controls in parallel. Treatments were in triplicate where indicated. Apoptosis experiments were performed as previously described (24) and analyzed on a BD LSR III (Becton Dickenson). The number of cells in quadrants II and IV (Annexin positive) were counted as apoptotic.

Cell Cycle

Cells were seeded at roughly 30–40% confluency and were treated overnight with the indicated treatments in triplicate, with no-treatment controls in parallel and the cells were prepared for cell cycle analysis as previously described (24) and analyzed on a BD LSR III (Becton Dickenson).

siRNA Experiments

For the siRNA experiments, *MCL-1* and scrambled control oligos (Dharmacon smart pool) were used at a concentration of 50nM and transfected with Hiperfect reagent (Qiagen). Briefly, cells were plated to achieve next day confluency of roughly 60% confluency. 75uL of Hiperfect was added to 750uL of OPTI-MEM in a 1.5mL eppendorf tube. In parallel, 10nM of siRNA was added to 750uL of Opti-MEM in a separate 1.5mL eppendorf tube. After ten minutes, the tubes were combined and mixed gently. Following ten more minutes, the Hiperfect-siRNA mix was then drop-wise added to cells, and gently shaken for five minutes. 24 hours later, the cells were either re-seeded in 6-well plates and treated with the appropriate drug the following day, or lysed for Western blot analysis to determine the efficiency of the knockdown.

shRNA Experiments

For the shRNA experiments, cells were transduced with tetracycline-inducible shKRAS vectors as previously described (9). Following selection in 2ug/ml puromycin, cells were grown in Tet-approved FBS and knockdown was performed in the presence of 50ng/ml of doxycycline for 72 hours.

Protein Complex Immunoprecipitation

Following indicated drug treatments, cells were lysed in the same buffer as used for Western blotting. 20uL of protein A sepharose beads were added to 250–500μg of protein, and 5μg of either MCL-1 antibody (S-19, Santa Cruz technology) or BIM antibody (cat# 2819, Cell Signaling) were added to the lysates. Following overnight incubation with motion, the supernatant was collected and the cell pellets were washed three times with PBS.

Xenograft Studies

***KrasG12D* genetically engineered mouse model—**Homozygous mutant *APC* and heterozygous mutant *KRAS* G12D mice were generated as previously described[1].

Adenoviral Infection of Colonic Epithelium

Tumors were induced in the colons of $Apc^{-/-}$ $Kras^{G12D/+}$ mice by adenovirus expressing cre recombinase and followed by optical colonoscopy as previously described (42).

In vivo treatments

For the human xenografts, KM-12 (n=5 for treatment group) or SW620 cells (n =4 for each cohort) were injected (5×10^6 cells per mouse) into the rear right flanks of athymic nude mice (Charles River Laboratories). When tumors reached approximately $100mm^3$ to $200mm^3$, treatments began. All drugs were administered directly to the stomach daily by oral gavage, unless otherwise indicated in the figure legend describing the data. For xenograft experiments, tumors were measured by electronic caliper two to three times a week, in two-dimensions (length and width), and with the formula : $v = l \times (w)2\ (\pi/6)$, where v = tumor volume, l = length, and w =width. For GEMMs, tumor size was determined by the Tumor Size Index (TSI) as calculated by (tumor area/colonic lumen area)×100 (%) (42).

All animal experiments were performed in accordance with Massachusetts General Hospital Animal Care or Tufts Institutional Animal Care and Use Committee.

Histopathology and immunohistochemistry

Tissue was fixed in 10% paraformaldehyde overnight, embedded in paraffin, and sectioned at the Department of Pathology, Massachusetts General Hospital. Cell death was determined by cleaved caspase 3 (CC3) positivity.

Statistical Considerations

IC50s for cell lines were calculated as previously described in the drug screens[6]. The Statistical tests used in this study were Student's *t*-test (two-sided) and Wilcoxon rank sum tests performed using Graphpad Prism Software or R version 2.14.1. Differences were considered statistically different if $P<0.05$. The average amount of apoptosis between all the mutant groups and all the wild-type groups, as described in the text, is +/− S.E.M.

Supplementary Material

Refer to Web version on PubMed Central for supplementary material.

Acknowledgments

Financial Support: This was work was supported by DF/HCC Gastrointestinal Cancer SPORE P50 CA127003 (J.A. Engelman), grants from the National Institute of Health: R01CA140594 (J.A. Engelman), R01CA137008 (J.A. Engelman), 1U54HG006097-01 (C.H. Benes), a grant from the Wellcome Trust (086357; C.H. Benes), awards from the Burroughs Wellcome Fund and the Howard Hughes Medical Institute (M.N.R.), and an American Cancer Society Postdoctoral Fellowship (A.C. Faber).

REFERENCES

1. Artale S, Sartore-Bianchi A, Veronese SM, Gambi V, Sarnataro CS, Gambacorta M, et al. Mutations of KRAS and BRAF in primary and matched metastatic sites of colorectal cancer. Journal of clinical oncology : official journal of the American Society of Clinical Oncology. 2008; 26:4217–4219. [PubMed: 18757341]
2. Vaughn CP, Zobell SD, Furtado LV, Baker CL, Samowitz WS. Frequency of KRAS, BRAF, and NRAS mutations in colorectal cancer. Genes, chromosomes & cancer. 2011; 50:307–312. [PubMed: 21305640]
3. Tian S, Simon I, Moreno V, Roepman P, Tabernero J, Snel M, et al. A combined oncogenic pathway signature of BRAF, KRAS and PI3KCA mutation improves colorectal cancer classification and cetuximab treatment prediction. Gut. 2013; 62:540–549. [PubMed: 22798500]
4. Yeh JJ, Routh ED, Rubinas T, Peacock J, Martin TD, Shen XJ, et al. KRAS/BRAF mutation status and ERK1/2 activation as biomarkers for MEK1/2 inhibitor therapy in colorectal cancer. Molecular cancer therapeutics. 2009; 8:834–843. [PubMed: 19372556]
5. Karapetis CS, Khambata-Ford S, Jonker DJ, O'Callaghan CJ, Tu D, Tebbutt NC, et al. K-ras mutations and benefit from cetuximab in advanced colorectal cancer. The New England journal of medicine. 2008; 359:1757–1765. [PubMed: 18946061]
6. Laurent-Puig P, Cayre A, Manceau G, Buc E, Bachet JB, Lecomte T, et al. Analysis of PTEN, BRAF, and EGFR status in determining benefit from cetuximab therapy in wild-type KRAS metastatic colon cancer. Journal of clinical oncology : official journal of the American Society of Clinical Oncology. 2009; 27:5924–5930. [PubMed: 19884556]
7. Siena S, Sartore-Bianchi A, Di Nicolantonio F, Balfour J, Bardelli A. Biomarkers predicting clinical outcome of epidermal growth factor receptor-targeted therapy in metastatic colorectal cancer. Journal of the National Cancer Institute. 2009; 101:1308–1324. [PubMed: 19738166]
8. Di Nicolantonio F, Martini M, Molinari F, Sartore-Bianchi A, Arena S, Saletti P, et al. Wild-type BRAF is required for response to panitumumab or cetuximab in metastatic colorectal cancer. Journal of clinical oncology : official journal of the American Society of Clinical Oncology. 2008; 26:5705–5712. [PubMed: 19001320]

9. Ebi H, Corcoran RB, Singh A, Chen Z, Song Y, Lifshits E, et al. Receptor tyrosine kinases exert dominant control over PI3K signaling in human KRAS mutant colorectal cancers. The Journal of clinical investigation. 2011; 121:4311–4321. [PubMed: 21985784]
10. Barbie DA, Tamayo P, Boehm JS, Kim SY, Moody SE, Dunn IF, et al. Systematic RNA interference reveals that oncogenic KRAS-driven cancers require TBK1. Nature. 2009; 462:108–112. [PubMed: 19847166]
11. Engelman JA, Chen L, Tan X, Crosby K, Guimaraes AR, Upadhyay R, et al. Effective use of PI3K and MEK inhibitors to treat mutant Kras G12D and PIK3CA H1047R murine lung cancers. Nature medicine. 2008; 14:1351–1356.
12. Halilovic E, She QB, Ye Q, Pagliarini R, Sellers WR, Solit DB, et al. PIK3CA mutation uncouples tumor growth and cyclin D1 regulation from MEK/ERK and mutant KRAS signaling. Cancer research. 2010; 70:6804–6814. [PubMed: 20699365]
13. Scholl C, Frohling S, Dunn IF, Schinzel AC, Barbie DA, Kim SY, et al. Synthetic lethal interaction between oncogenic KRAS dependency and STK33 suppression in human cancer cells. Cell. 2009; 137:821–834. [PubMed: 19490892]
14. Singh A, Sweeney MF, Yu M, Burger A, Greninger P, Benes C, et al. TAK1 inhibition promotes apoptosis in KRAS-dependent colon cancers. Cell. 2012; 148:639–650. [PubMed: 22341439]
15. Kumar MS, Hancock DC, Molina-Arcas M, Steckel M, East P, Diefenbacher M, et al. The GATA2 transcriptional network is requisite for RAS oncogene-driven non-small cell lung cancer. Cell. 2012; 149:642–655. [PubMed: 22541434]
16. Corcoran RBCK, Ebi H, Hata A, Faber AC, Coffee EM, Greninger P, Brown RD, Godfrey JT, Cohoon TJ, Song Y, Lifshits E, Hung KE, Shioda T, Dias-Santagata D, Singh A, Settleman J, Benes CH, Mino-Kenudson M, Wong KK, Engelman JA. Synthetic lethal interaction of combined BCL-XL and MEK inhibition promotes tumor regressions in KRAS mutant cancer models. in press.
17. Davies H, Bignell GR, Cox C, Stephens P, Edkins S, Clegg S, et al. Mutations of the BRAF gene in human cancer. Nature. 2002; 417:949–954. [PubMed: 12068308]
18. Popovici V, Budinska E, Tejpar S, Weinrich S, Estrella H, Hodgson G, et al. Identification of a poorprognosis BRAF-mutant-like population of patients with colon cancer. Journal of clinical oncology : official journal of the American Society of Clinical Oncology. 2012; 30:1288–1295. [PubMed: 22393095]
19. Tol J, Nagtegaal ID, Punt CJ. BRAF mutation in metastatic colorectal cancer. The New England journal of medicine. 2009; 361:98–99. [PubMed: 19571295]
20. Flaherty KT, Puzanov I, Kim KB, Ribas A, McArthur GA, Sosman JA, et al. Inhibition of mutated, activated BRAF in metastatic melanoma. The New England journal of medicine. 2010; 363:809–819. [PubMed: 20818844]
21. Prahallad A, Sun C, Huang S, Di Nicolantonio F, Salazar R, Zecchin D, et al. Unresponsiveness of colon cancer to BRAF(V600E) inhibition through feedback activation of EGFR. Nature. 2012; 483:100–103. [PubMed: 22281684]
22. Corcoran RB, Ebi H, Turke AB, Coffee EM, Nishino M, Cogdill AP, et al. EGFR-mediated re-activation of MAPK signaling contributes to insensitivity of BRAF mutant colorectal cancers to RAF inhibition with vemurafenib. Cancer discovery. 2012; 2:227–235. [PubMed: 22448344]
23. Garnett MJ, Edelman EJ, Heidorn SJ, Greenman CD, Dastur A, Lau KW, et al. Systematic identification of genomic markers of drug sensitivity in cancer cells. Nature. 2012; 483:570–575. [PubMed: 22460902]
24. Faber AC, Corcoran RB, Ebi H, Sequist LV, Waltman BA, Chung E, et al. BIM expression in treatment-naive cancers predicts responsiveness to kinase inhibitors. Cancer discovery. 2011; 1:352–365. [PubMed: 22145099]
25. Faber AC, Ebi H, Costa C, Engelman JA. Apoptosis In Targeted Therapy Responses: The Role of BIM. Adv Pharmacol. 2012; 65:519–542. [PubMed: 22959036]
26. Brachmann SM, Hofmann I, Schnell C, Fritsch C, Wee S, Lane H, et al. Specific apoptosis induction by the dual PI3K/mTor inhibitor NVP-BEZ235 in HER2 amplified and PIK3CA mutant breast cancer cells. Proceedings of the National Academy of Sciences of the United States of America. 2009; 106:22299–22304. [PubMed: 20007781]

27. Yang W, Soares J, Greninger P, Edelman EJ, Lightfoot H, Forbes S, et al. Genomics of Drug Sensitivity in Cancer (GDSC): a resource for therapeutic biomarker discovery in cancer cells. Nucleic acids research. 2013; 41:D955–D961. [PubMed: 23180760]

28. Tse C, Shoemaker AR, Adickes J, Anderson MG, Chen J, Jin S, et al. ABT-263: a potent and orally bioavailable Bcl-2 family inhibitor. Cancer research. 2008; 68:3421–3428. [PubMed: 18451170]

29. Shoemaker AR, Mitten MJ, Adickes J, Ackler S, Refici M, Ferguson D, et al. Activity of the Bcl-2 family inhibitor ABT-263 in a panel of small cell lung cancer xenograft models. Clinical cancer research : an official journal of the American Association for Cancer Research. 2008; 14:3268–3277. [PubMed: 18519752]

30. Gandhi L, Camidge DR, Ribeiro de Oliveira M, Bonomi P, Gandara D, Khaira D, et al. Phase I study of Navitoclax (ABT-263), a novel Bcl-2 family inhibitor, in patients with small-cell lung cancer and other solid tumors. Journal of clinical oncology : official journal of the American Society of Clinical Oncology. 2011; 29:909–916. [PubMed: 21282543]

31. Roberts AW, Seymour JF, Brown JR, Wierda WG, Kipps TJ, Khaw SL, et al. Substantial susceptibility of chronic lymphocytic leukemia to BCL2 inhibition: results of a phase I study of navitoclax in patients with relapsed or refractory disease. Journal of clinical oncology : official journal of the American Society of Clinical Oncology. 2012; 30:488–496. [PubMed: 22184378]

32. Nguyen M, Marcellus RC, Roulston A, Watson M, Serfass L, Murthy Madiraju SR, et al. Small molecule obatoclax (GX15-070) antagonizes MCL-1 and overcomes MCL-1-mediated resistance to apoptosis. Proceedings of the National Academy of Sciences of the United States of America. 2007; 104:19512–19517. [PubMed: 18040043]

33. Paik PK, Rudin CM, Pietanza MC, Brown A, Rizvi NA, Takebe N, et al. A phase II study of obatoclax mesylate, a Bcl-2 antagonist, plus topotecan in relapsed small cell lung cancer. Lung Cancer. 2011; 74:481–485. [PubMed: 21620511]

34. Hwang JJ, Kuruvilla J, Mendelson D, Pishvaian MJ, Deeken JF, Siu LL, et al. Phase I dose finding studies of obatoclax (GX15-070), a small molecule pan-BCL-2 family antagonist, in patients with advanced solid tumors or lymphoma. Clinical cancer research : an official journal of the American Association for Cancer Research. 2010; 16:4038–4045. [PubMed: 20538761]

35. Schimmer AD, O'Brien S, Kantarjian H, Brandwein J, Cheson BD, Minden MD, et al. A phase I study of the pan bcl-2 family inhibitor obatoclax mesylate in patients with advanced hematologic malignancies. Clinical cancer research : an official journal of the American Association for Cancer Research. 2008; 14:8295–8301. [PubMed: 19088047]

36. Wendel HG, Silva RL, Malina A, Mills JR, Zhu H, Ueda T, et al. Dissecting eIF4E action in tumorigenesis. Genes & development. 2007; 21:3232–3237. [PubMed: 18055695]

37. Hsieh AC, Costa M, Zollo O, Davis C, Feldman ME, Testa JR, et al. Genetic dissection of the oncogenic mTOR pathway reveals druggable addiction to translational control via 4EBP-eIF4E. Cancer cell. 2010; 17:249–261. [PubMed: 20227039]

38. Mills JR, Hippo Y, Robert F, Chen SM, Malina A, Lin CJ, et al. mTORC1 promotes survival through translational control of Mcl-1. Proceedings of the National Academy of Sciences of the United States of America. 2008; 105:10853–10858. [PubMed: 18664580]

39. Faber AC, Li D, Song Y, Liang MC, Yeap BY, Bronson RT, et al. Differential induction of apoptosis in HER2 and EGFR addicted cancers following PI3K inhibition. Proceedings of the National Academy of Sciences of the United States of America. 2009; 106:19503–19508. [PubMed: 19850869]

40. Schatz JH, Oricchio E, Wolfe AL, Jiang M, Linkov I, Maragulia J, et al. Targeting cap-dependent translation blocks converging survival signals by AKT and PIM kinases in lymphoma. The Journal of experimental medicine. 2011; 208:1799–1807. [PubMed: 21859846]

41. Chresta CM, Davies BR, Hickson I, Harding T, Cosulich S, Critchlow SE, et al. AZD8055 is a potent, selective, and orally bioavailable ATP-competitive mammalian target of rapamycin kinase inhibitor with in vitro and in vivo antitumor activity. Cancer research. 2010; 70:288–298. [PubMed: 20028854]

42. Hung KE, Maricevich MA, Richard LG, Chen WY, Richardson MP, Kunin A, et al. Development of a mouse model for sporadic and metastatic colon tumors and its use in assessing drug treatment.

Proceedings of the National Academy of Sciences of the United States of America. 2010; 107:1565–1570. [PubMed: 20080688]

43. Martin ES, Belmont PJ, Sinnamon MJ, Richard LG, Yuan J, Coffee EM, et al. Development of a colon cancer GEMM-derived orthotopic transplant model for drug discovery and validation. Clinical cancer research : an official journal of the American Association for Cancer Research. 2013; 19:2929–2940. [PubMed: 23403635]
44. Shirasawa S, Furuse M, Yokoyama N, Sasazuki T. Altered growth of human colon cancer cell lines disrupted at activated Ki-ras. Science. 1993; 260:85–88. [PubMed: 8465203]
45. She QB, Halilovic E, Ye Q, Zhen W, Shirasawa S, Sasazuki T, et al. 4E-BP1 is a key effector of the oncogenic activation of the AKT and ERK signaling pathways that integrates their function in tumors. Cancer cell. 2010; 18:39–51. [PubMed: 20609351]
46. Del Gaizo Moore V, Brown JR, Certo M, Love TM, Novina CD, Letai A. Chronic lymphocytic leukemia requires BCL2 to sequester prodeath BIM, explaining sensitivity to BCL2 antagonist ABT-737. The Journal of clinical investigation. 2007; 117:112–121. [PubMed: 17200714]
47. Sale MJ, Cook SJ. The BH3 mimetic ABT-263 synergizes with the MEK1/2 inhibitor selumetinib/AZD6244 to promote BIM-dependent tumour cell death and inhibit acquired resistance. The Biochemical journal. 2013; 450:285–294. [PubMed: 23234544]
48. Kuraguchi M, Wang XP, Bronson RT, Rothenberg R, Ohene-Baah NY, Lund JJ, et al. Adenomatous polyposis coli (APC) is required for normal development of skin and thymus. PLoS genetics. 2006; 2:e146. [PubMed: 17002498]
49. Steckel M, Molina-Arcas M, Weigelt B, Marani M, Warne PH, Kuznetsov H, et al. Determination of synthetic lethal interactions in KRAS oncogene-dependent cancer cells reveals novel therapeutic targeting strategies. Cell research. 2012; 22:1227–1245. [PubMed: 22613949]
50. Luo J, Emanuele MJ, Li D, Creighton CJ, Schlabach MR, Westbrook TF, et al. A genome-wide RNAi screen identifies multiple synthetic lethal interactions with the Ras oncogene. Cell. 2009; 137:835–848. [PubMed: 19490893]

Significance

Effective targeted therapies directed against CRC with activating mutations in *KRAS* remains elusive. We have leveraged drug screen data from a large panel of human CRCs to uncover an effective, rational targeted therapy strategy that has preferential activity in CRCs with *KRAS* or *BRAF* mutations. This combination may be developed for clinical testing.

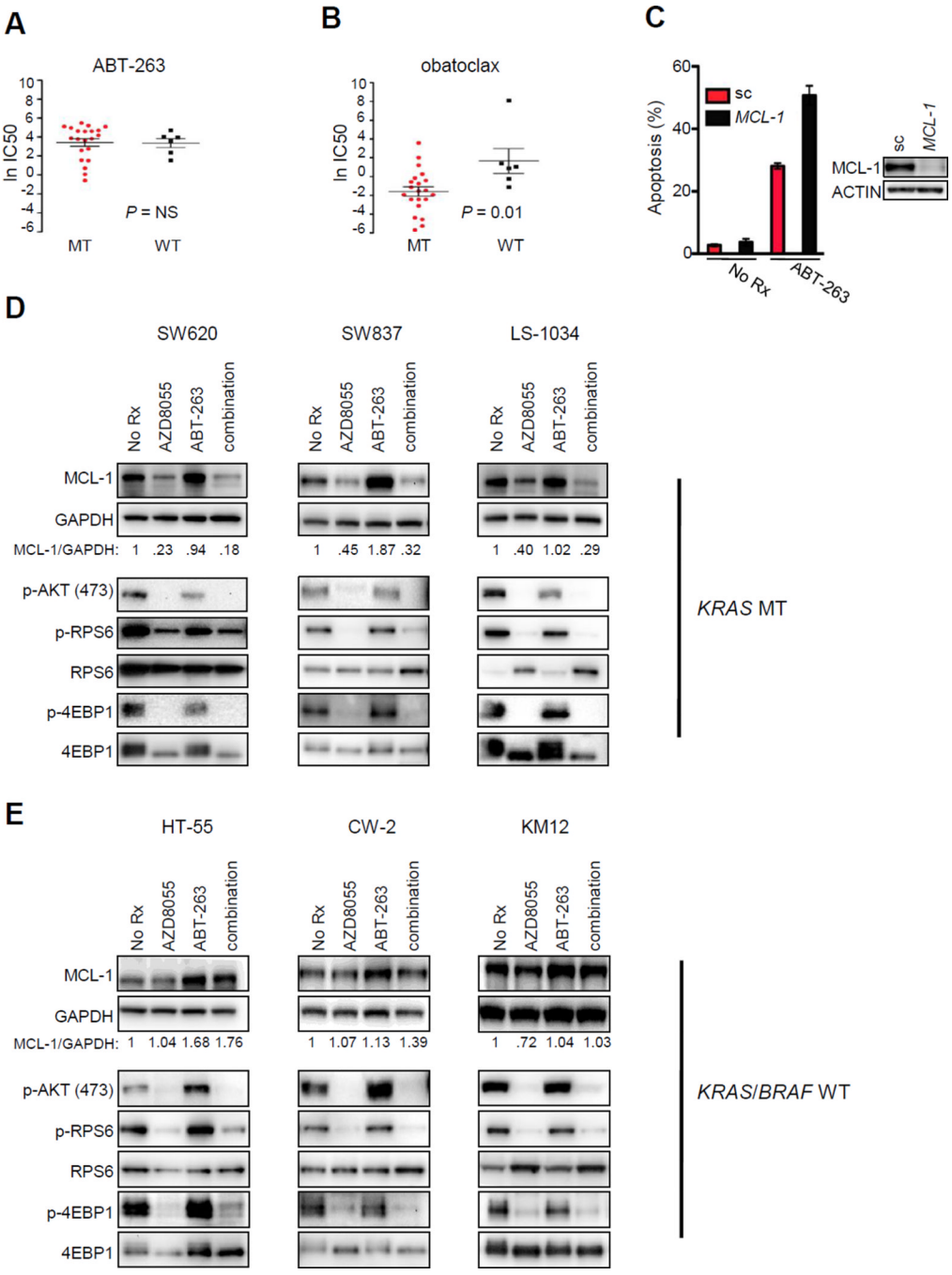

Figure 1. *KRAS* and *BRAF* mutant colorectal cancers have increased sensitivity to obatoclax compared to their wild-type counterparts and also have MCL-1 expression under the regulation of TORC1/2

KRAS mutant (MT), *BRAF* MT, and wild-type (WT) colorectal cells were treated with increasing concentrations of (A) the BCL-2/XL inhibitor ABT-263 or (B) the BCL-2/XL/MCL-1 inhibitor obatoclax for 72 hours; cell number was determined, and IC50s were calculated (and converted to natural log, y axis). Student's t tests were performed between the two groups (*KRAS* or *BRAF* MT versus WT) and *P* values were determined (NS=not significant) (n=27). (C) *KRAS* MT SW620 cells were transfected with 50 nM scrambled (sc) or 50 nM *MCL-1* siRNA for 24 hours. An aliquot of transfected cells was used to prepare

lysates for Western blot analyses with the indicated antibodies (lower panels) or re-seeded and the next day treated for 48 hours with vehicle (no Rx) or 1 μM ABT-263; percent of apoptotic cells was quantified by FACS (n=3). (D) *KRAS* MT or (E) *KRAS/BRAF* WT colorectal cell lines were treated for 16 hours with no drug (No Rx), 500 nM AZD8055, 1 μM ABT-263, or combination AZD8055/ABT-263, and proteins from lysates were subjected to Western blot analyses with the indicated antibodies. The numbers in the panels represent the amount of MCL-1 normalized to GAPDH. The detection of MCL-1 and GAPDH were performed on the same membrane.

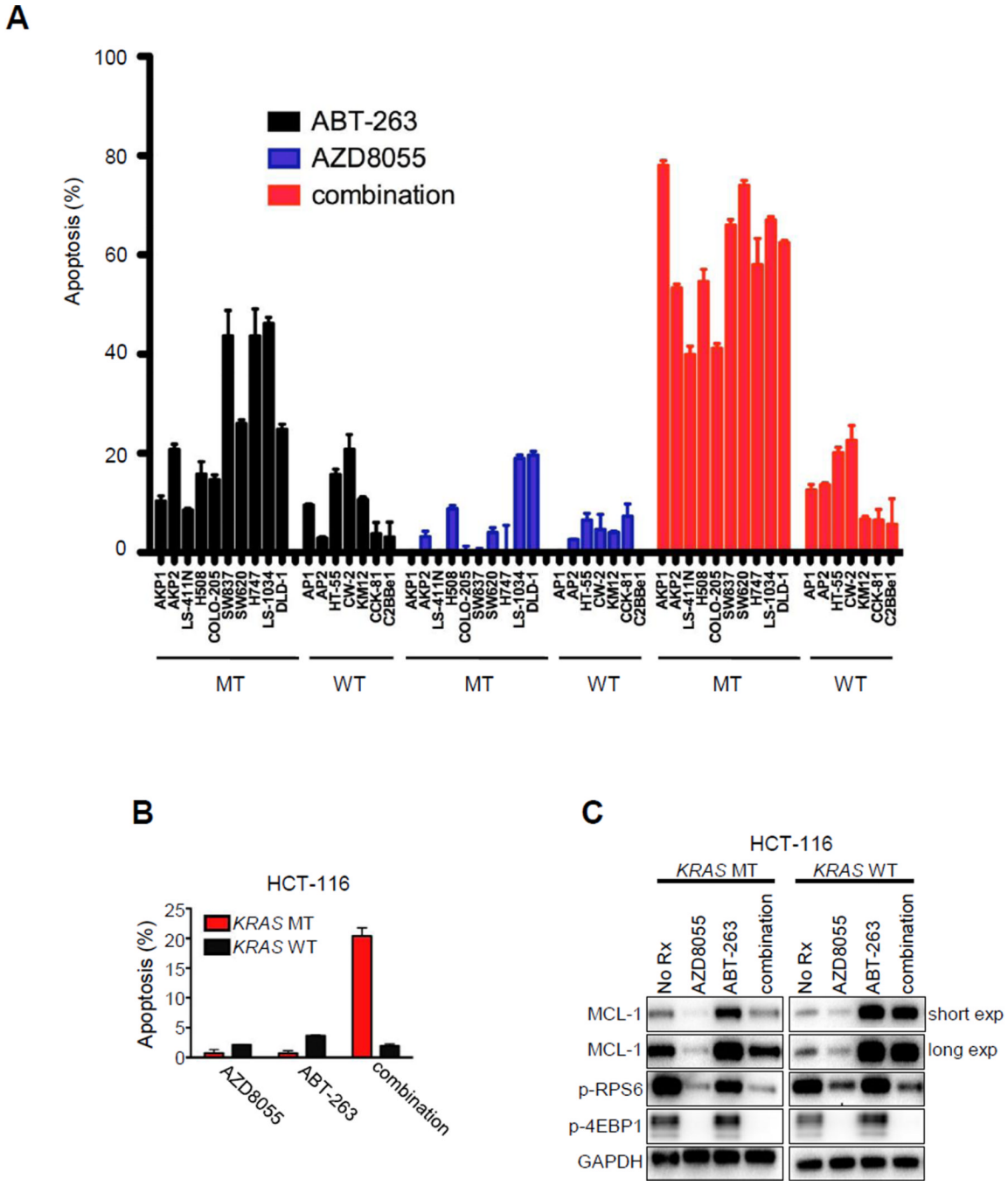

Figure 2. Increased induction of apoptosis in *KRAS* and *BRAF* mutant colorectal cancers treated with combined ABT-263/AZD8055 compared to *KRAS/BRAF* wild-type colorectal cancers

(A) The indicated cell lines were treated with no drug, 500 nM AZD8055, 1 μM ABT-263, or combination AZD8055/ABT-263 for 72 hours. Percent of apoptotic cells was quantified by FACS. Each bar graph represents the amount of apoptosis induced by treatment relative to no drug treatment. Error bars are the S.D. (n=3). Mutant (MT) cell lines consist of *KRAS* or *BRAF* MT human CRC cell lines, as well as CRC cell lines derived from a *KRAS* MT genetically-engineered mouse model (GEMM) (AKP1 and AKP2). Wild-type (WT) cells consist of *KRAS/BRAF* WT human CRC cell lines as well as CRC cell lines derived from a *KRAS* WT GEMM (AP1 and AP2). (B and C) Isogenic HCT-116 cells that were either

KRAS MT or WT were treated with no drug (No Rx), 500 nM AZD8055, 1 μM ABT-263, or the combination of ABT-263/AZD8055 (263/8055) for (B) 72 hours and the percent of apoptotic cells was quantified by FACS, or (C) overnight and proteins from lysates were subjected to Western blot analyses with the indicated antibodies. For (B), each bar graph represents the amount of apoptosis induced by treatment relative to no drug treatment. Error bars are the S.D. (n=3).

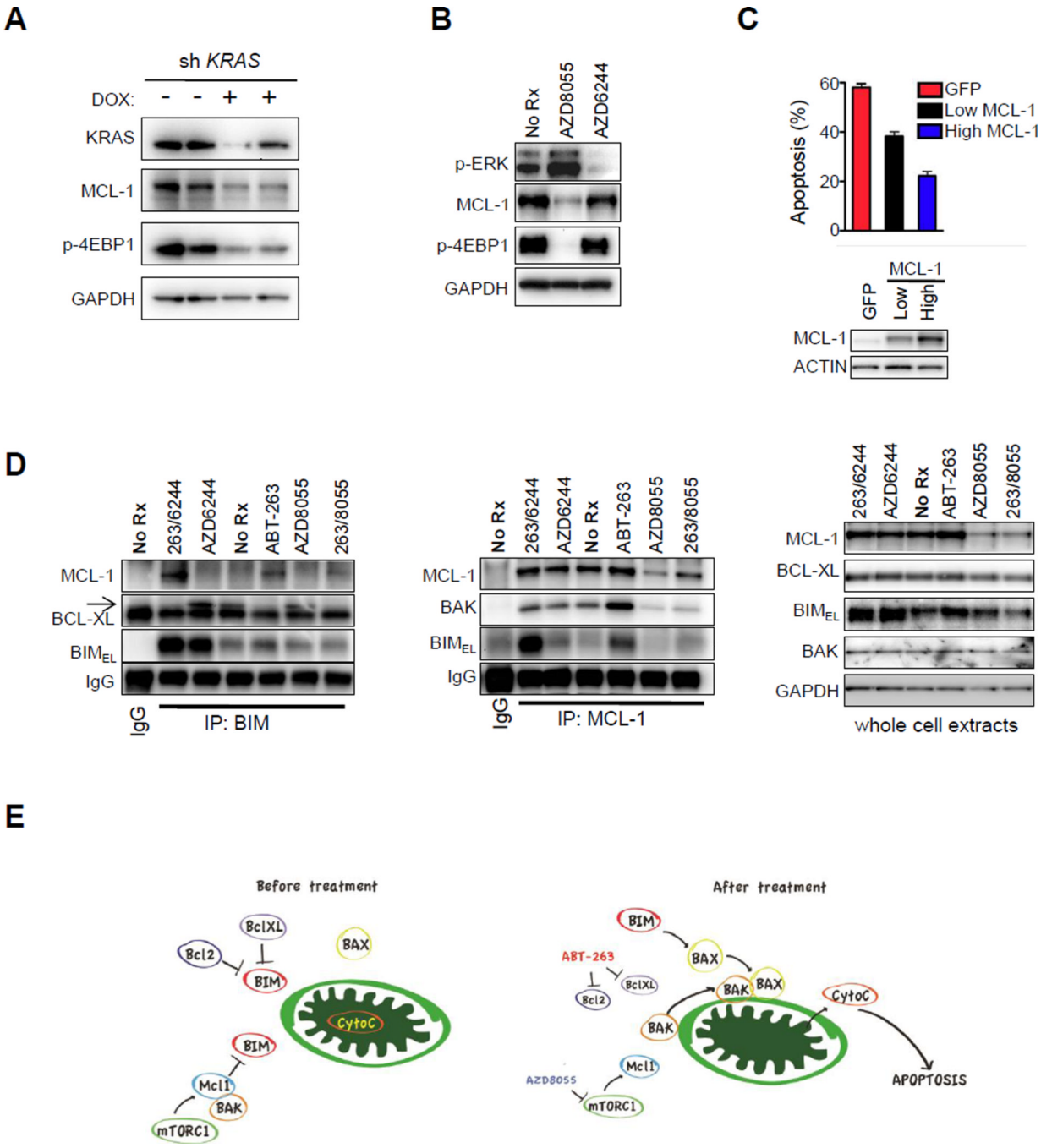

Figure 3. TORC inhibition, but not MEK inhibition, downregulates MCL-1 and disrupts MCL-1:BIM complexes following ABT-263 therapy, leading to enhanced apoptosis

(A) *KRAS* MT SW620 colorectal cells expressing doxycycline-inducible KRAS shRNA vectors were treated with or without 50 ng/mL doxycycline (DOX) for 72 hours, and lysates were subjected to Western blot analyses with the indicated antibodies. (B) *KRAS* MT SW620 colorectal cells were treated for 16 hours with no drug (no Rx), 500 nM AZD8055, or 1 μM AZD6244, and lysates were subjected to Western blot analyses with the indicated antibodies. (C) Stable clones of SW620 cells expressing GFP alone or a GFP-IRES-MCL-1 were sorted by FACS by fluorescence intensity and the populations of cells were separated. Western blot analyses of the resultant cell lines are shown in the lower panel. Cells were

treated for 72 hours with the ABT-263/AZD8055 combination therapy and apoptosis was determined by FACS. Each bar graph represents the amount of apoptosis induced by treatment relative to no drug treatment. Error bars are the S.D. (n=3). (D) SW620 parental cells underwent immunoprecipitation (IP) with antibodies targeting BIM (left panel), MCL-1 (middle panel), or IgG (left and middle panels) following six hours of no drug (no Rx), 500 nM AZD8055, 1 μM ABT-263, combination therapy (263/8055), 1 μM AZD6244, or combination of AZD6244 and ABT-263 (263/6244). Precipitates were analyzed by Western blot analyses with the indicated antibodies. Arrow indicates BCL-XL that migrates slower than the light chain. Whole cell lysates were set aside prior to IP and were subjected to Western blot analyses with the indicated antibodies (right panel). (E) The schematic displays how ABT-263 and AZD8055 combination therapy affect the balance of BCL-2 family proteins to induce apoptosis in *KRAS* MT cells. Mitochondria are depicted in green.

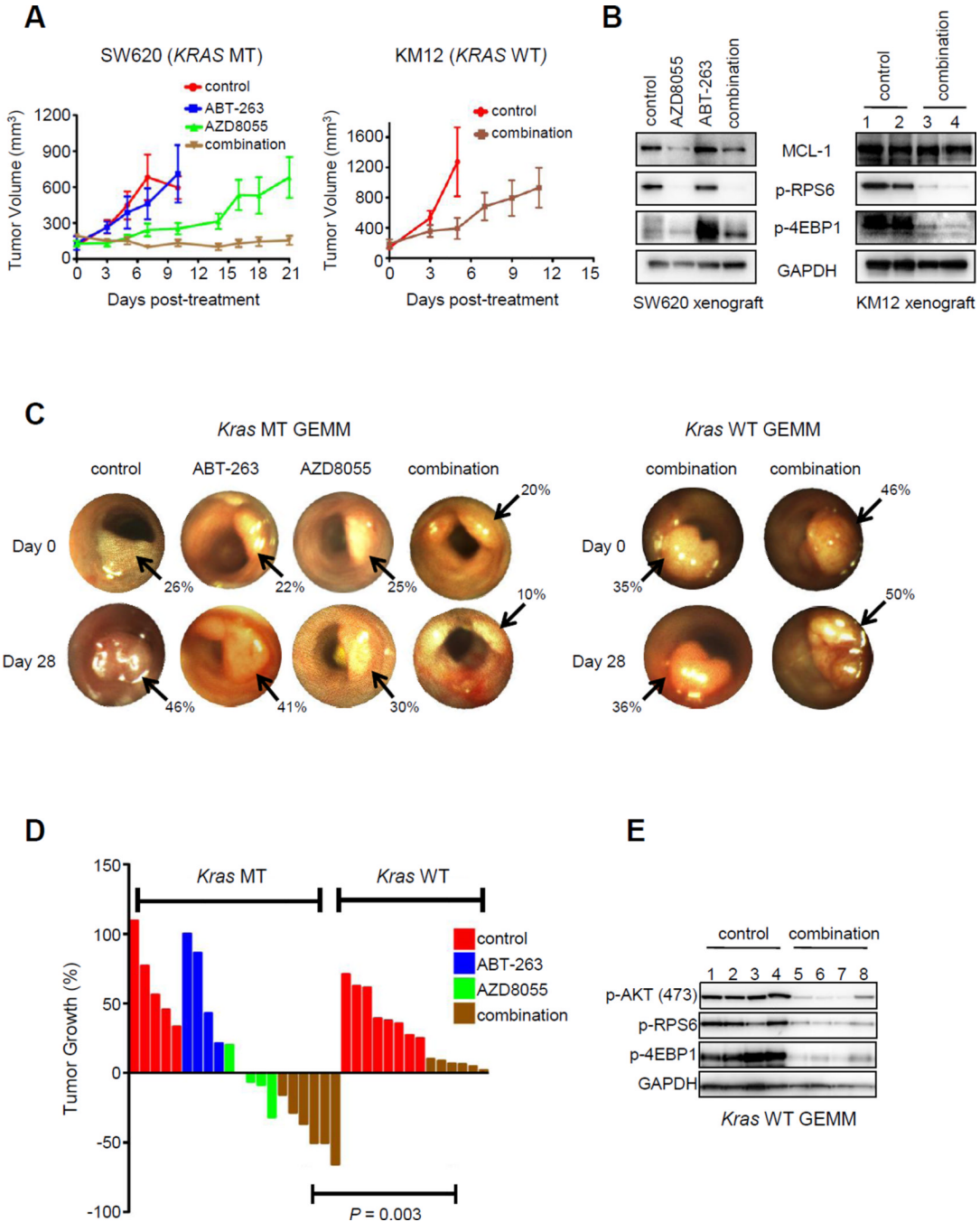

Figure 4. The combination of AZD8055/ABT-263 has *in vivo* efficacy in *KRAS* mutant CRC

(A) Cohorts of *KRAS* MT SW620 xenograft tumors (left panel) were treated with no drug (control), AZD8055 (16 mg/kg/qd), ABT-263 (80 mg/kg/qd), or the combination (16 mg/kg/qd AZD8055, 80 mg/kg/qd ABT-263). Average tumor sizes for each treatment group are plotted. Cohorts of *KRAS* wild-type KM12 xenograft tumors (right panel) were treated with vehicle control or AZD8055/ABT-263 combination, and average tumor sizes are plotted. (B) Approximately three hours following the final drug treatment, mice were euthanized and tumors were harvested. Protein lysates were prepared from SW620 (left) and KM12 (right) tumors and were subjected to Western blot analyses with the indicated antibodies. (C)

Representative images of tumors taken from serial colonoscopies of *KRAS* MT and *KRAS* WT GEMMs as treated in (A). Arrows depict each tumor. Tumor size was calculated by determining the percent occlusion of the lumen as described in Materials and Methods. (D) Colorectal cancers in *KRAS* MT and *KRAS* WT GEMMs were treated as in (A) for 28 days and changes in tumor volume for each mouse are shown by a waterfall plot. (E) Lysates from *KRAS* WT GEMM tumors were harvested approximately three hours following the last drug treatment of the experiment, and protein lysates were subjected to Western blotting analyses with the indicated antibodies. Each number represents a different tumor.